

Fabian Waleffe^{1†} and John Kim^{2‡§}

¹ Mathematics and Engineering Physics Departments, University of Wisconsin, Madison, WI 53706-1313

² Mechanical and Aerospace Engineering Department, University of California, Los Angeles, CA 90095-1597

Abstract

This article is a follow-up on our contribution, under a similar title, to the monograph on “Self-Sustaining Mechanisms of Wall Turbulence” (R. Panton, Ed. Computational Mechanics Publications, 1997). Here, we present further evidence of the validity and relevance of the self-sustaining process that we have demonstrated in earlier publications. In particular, we show exact steady state solutions, calculated using our understanding of the self-sustaining process, that are strikingly similar to the coherent structures observed in the near-wall region of turbulent shear flows. We take this opportunity to further relate our approach to other studies and to answer some criticisms advanced by others in the cited monograph.

1 Introduction

Various conceptual models and sketches have been proposed to explain the origin and dynamics of the coherent structures observed in wall-bounded turbulence [1]. These pictures are often very descriptive, sometime rather complicated, but usually have little contact with the governing Navier-Stokes equations. This leaves plenty of room for controversies and arguments. One issue, for instance, has been the role of the interaction between the outer flow – the region beyond $y_+ \approx 50$ – and the near-wall flow where the coherent structures reside primarily. A key question is whether that interaction is crucial to the maintenance of wall-bounded turbulence. Another question is whether the mechanisms at play are of inviscid or viscous origin. Some frequently cited concepts remain ill-defined, such as the distinction between “active” and “inactive” motions. Everyone now seems to agree that low-speed streaks and streamwise vortices are essential ingredients of the coherent structures and the dynamics of the near-wall region, but the meaning of “streamwise vortices” varies among authors. Another lasting debate has been whether symmetric “hairpin” structures or asymmetric staggered vortices, as shown

in Fig. 1, are the dominant structures.

Our work answers several of these questions using the Gordian knot strategy: for some of our results there is no outer flow, no viscous mechanism possible, only one type of structure is allowed and there are no inactive motions. In fact, some of the results correspond to non-trivial steady states for which there is no turbulence at all! Yet, those states are strikingly similar to the observed coherent structures and display the principal ingredients referred to by most researchers.

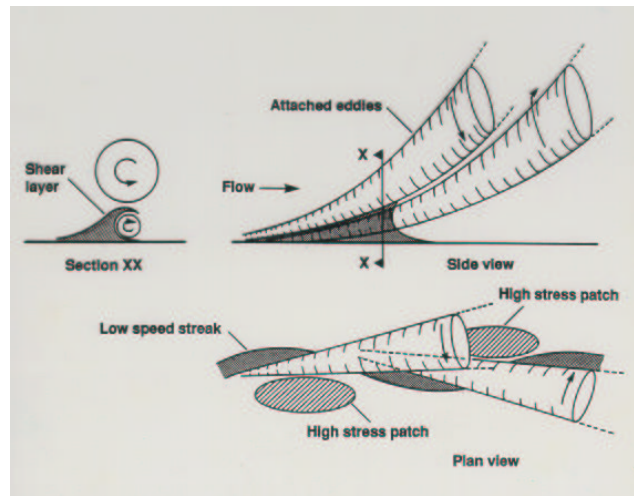


Figure 1: Sketch of the coherent structure educed from DNS data, from Stretch [2], see also [3].

2 Self-Sustaining Process

The process that we have studied involves streamwise rolls, a streaky shear flow and an x -dependent streak instability. As usual, we use (x, y, z) for the streamwise, wall-normal, and spanwise coordinates, respectively, and (u, v, w) for the corresponding velocity components. By streamwise rolls, we mean a motion of the form $[0, V(y, z), W(y, z)]$ that is x -independent and with no x -velocity component (the time dependence is kept implicit). The streaky flow is a 1-component, 2-dimensional flow of the form $[U(y, z), 0, 0]$ which consists of the usual mean flow $\bar{U}(y)$ and streamwise streaks $[U(y, z) - \bar{U}(y), 0, 0]$. “Streamwise streaks” thus refers to the x -averaged streamwise velocity fluctuation. The x -dependent streak instability mode is a 3-dimensional, 3-component divergence-free field with zero x -average.

*Presented by invitation at the 29th AIAA Fluid Dynamics Conference, Albuquerque, New Mexico, June 15-18, 1998; AIAA Paper 98-2997.

[†]Assistant Professor

[‡]Professor, Associate Fellow

[§]Copyright ©1998 by Waleffe and Kim. Published by the American Institute of Aeronautics and Astronautics, Inc., with permission.

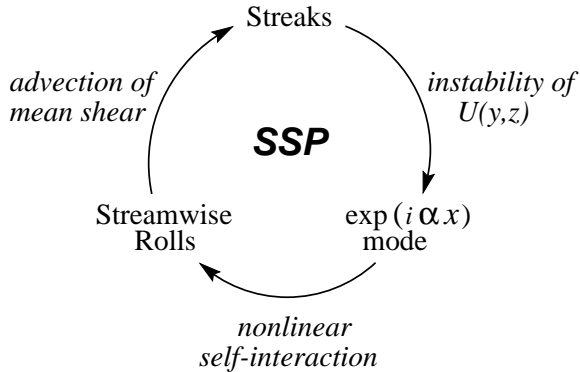


Figure 2: The Self-Sustaining Process.

We have demonstrated that these various elements are linked through a complete cause-effect loop that constitutes the self-sustaining process [4, 5, 6, 7]. In this process, the streamwise rolls redistribute the mean shear to create streaks, the streaks are unstable through an instability of inflectional type (“wake-like”) and the nonlinear self-interaction of the 3D perturbation that results from that instability directly feeds back onto the rolls. These various phases have been discussed in details in earlier publications [6, 7].

The self-sustaining process, as sketched in Fig. 2, has a weakly nonlinear flavor. For sustenance (in a steady state or statistically steady state sense), rolls of $O(R^{-1})$ are sufficient to overcome the viscous dissipation of $O(1)$ streaks, and the quadratic nonlinear self-interaction of an $O(R^{-1})$ streak eigenmode is in turn sufficient to balance the viscous dissipation of the $O(R^{-1})$ rolls¹. Thus for sufficiently large Reynolds number R , the rolls and streak eigenmode are of small amplitude while the streaks are of $O(1)$. This is in the spirit of the “Mean Flow-First Harmonic theory” proposed by Benney [8] which was an important inspiration for our work (at least to the first author).

A key ingredient of the self-sustaining process is the instability of the streaky flow $[U(y, z), 0, 0]$ (Benney’s “Mean Flow”) which we studied through DNS [4] and eigenmode analysis [5, 6]. That instability is clearly driven by the spanwise inflections but the mean shear is crucial to shaping the eigenmode in such a way that feedback on the rolls does occur [6, 7]. To further investigate the streak instability, we have performed 3-dimensional eigenmode analyses for the linear stability of the streaks $[U(y, z) - \bar{U}(y), 0, 0]$, the streaky flow $[U(y, z), 0, 0]$, and the full x -independent flow $[U(y, z), V(y, z), W(y, z)]$.

The 2-dimensional streaks are strongly unstable to a 3D perturbation of sinusoidal type (see Sect. 4). A plot of the growth rate of that instability *vs.* streamwise wavenumber α has a form typical of inflectional instabilities (dash-dot curve in Fig. 4). In particular, the insta-

¹These scalings are for the “lower branch” of sustained states only, see [6], Sect. III D.

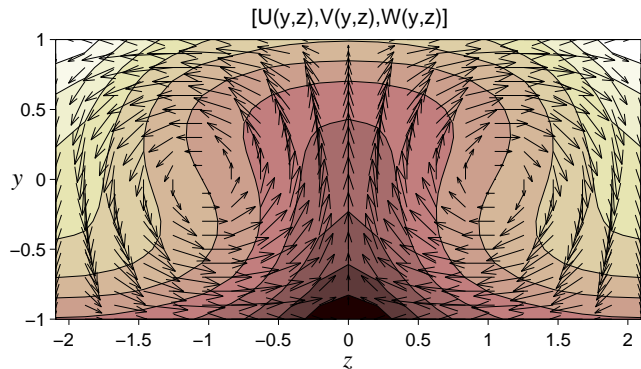


Figure 3: The 2-dimensional streaky base field for imposed stress boundary conditions with $\gamma = 1.50$, $R = 150$ and streamwise rolls with $V_{\max} = 0.05$ at $y = 0$, $z = 0$. Contours of U from minimum of -0.7 at $y = -1$, $z = 0$ to maximum of 0.7 at $y = 1$, $z = \pi/\gamma$ by steps of 0.1167 . Velocity arrows for V , W .

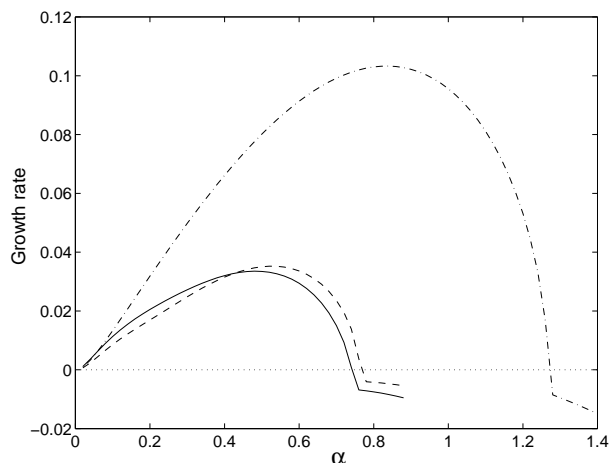


Figure 4: Growth rate of 3D instability of $[U(y, z) - \bar{U}(y), 0, 0]$ (dash-dot), $[U(y, z), 0, 0]$ (dash) and $[U(y, z), V(y, z), W(y, z)]$ (solid) for fields of Fig. 3.

bility takes place for wavenumbers $\alpha < \gamma$, where γ is the spanwise wavenumber [5]. Addition of the mean shear to the streaks strongly reduces the instability (dashed curve in Fig. 4). Addition of the rolls (solid curve in Fig. 4), further *reduces* the growth rate for $\alpha > 0.425$. This implies, because of conservation of energy by the nonlinear term in the Navier-Stokes equations, that the instability is driven by the streaks but that the “Reynolds stresses” of the eigenmode actually put energy *into* both the mean and the rolls. This is in complete agreement with a low-order model discussed elsewhere [6] and is an indirect verification that the nonlinear interaction of the streak eigenmode regenerates the rolls.

Figure 4 shows that the rolls enhance the instability of the streaky flow (solid *vs.* dash in Fig. 4) at small x -wavenumber α , hence they lose energy to the 3D mode for those α ’s. It is only for $\alpha > 0.425$ that the rolls

reduce the instability and hence receive energy. The mean shear has a major stabilizing effect but it is crucial to feedback on the rolls as discussed in [6, 7].

3 Relation to other studies

The relevance of instabilities arising from spanwise inflections has been emphasized by Blackwelder and collaborators [9] who have used the Gortler flow geometry to study the breakdown of streaky flows. The concave wall in the Gortler flow provides a linear instability mechanism (the centrifugal instability) that introduces streamwise vortices. The latter create streaks by the simple advection of the mean shear. The streaks then breakdown and a transition to full-blown turbulence follows. Although closely related to the process we studied, this approach has not been able to demonstrate a complete self-sustaining process. Such a demonstration would require getting rid of the concave wall and showing that a principal component of the “breakdown” is to feedback on the streamwise rolls. Nonetheless, we completely agree with the idea that an instability resulting from the spanwise inflection is a key element of the self-sustaining process.

We note here that other authors have used approaches similar to the Gortler flow model. Malkus and Zaff [10] considered pressure-driven *narrow-gap Ekman flow* as a model of plane Poiseuille flow. Nagata [11] considered *narrow-gap Taylor-Couette flow* and Clever and Busse [12] considered *sheared convection* as models of plane Couette flow. Each of these different settings has the same effect: they all provide a linear instability mechanism that introduces streamwise vortices. The important extra aspect of these works however, is that they succeeded in tracking sustained nonlinear states back to the pure plane geometry where there is no linear mechanism to sustain the streamwise rolls (system rotation or heating from below are easier to control than the concavity of walls).

Our focus has been to demonstrate a complete self-sustaining process and in particular to elucidate the nonlinear mechanism that sustains the streamwise vortices. We have shown that streamwise vortices directly result from the nonlinear self-interaction of the 3D perturbation that develops from the streaky flow instability and that those streamwise vortices have the right shape to in turn sustain the streaky flow [4, 5, 6, 7]. We emphasize that this feedback on the rolls is direct. We have demonstrated it explicitly and do not call on a broadband “burst” as in the models developed by Landahl [13]. The basis of Landahl’s model is the formation of streaks through what he calls the lift-up mechanism. That part is very similar to the formation of streaks through the redistribution of the mean shear by streamwise rolls in the process of Fig. 2. Landahl emphasizes that the elongated streaks arise from localized disturbances in his model, but the vertical velocity component

v of those localized disturbances must have a non-zero x -average. This is equivalent to our focus on x -averaged streamwise rolls as a key element of the self-sustaining process (see further discussion in the next section). In Landahl’s work, the crucial feedback on the original disturbance that leads to streaks is modelled as a highly intermittent nonlinear driving term (in the form of Dirac delta functions in time) which he envisions as resulting from inflectional instabilities (of unspecified origin). In contrast, we explicitly demonstrate that the Reynolds stresses of the 3D disturbance that results from the instability of the streaky flow do regenerate our original streamwise rolls, so no modelling is necessary. The process we studied is undoubtedly idealized. It applies to the canonical problems of long pipes and channels. Our goal is to clearly identify a complete process in the simplest setting. Once that is done, a new starting point is available to investigate other features of observed flows, such as spots and intermittency. The key point is that the process we studied is complete. It is fully consistent with, and indeed deduced from, the Navier-Stokes equations and does not require any modeling.

The sketches in Acarlar and Smith [14] which suggest the formation of horseshoe vortices through a Kelvin-Helmholtz type roll-up of a *two dimensional* shear layer (i.e. $[U(y, z), 0, 0]$) and the regeneration of the shear layer by the horseshoe, were another important inspiration for our work in addition to Benney’s ideas cited above. Our studies of the streaky flow instability have identified two main modes of instability, sinusoidal and varicose, as for the inflectional instabilities of wakes. In the very symmetric plane Couette flow, where high-speed streaks have the same strength as low-speed streaks, there are actually three possible types of streaky flow instability: fundamental sinusoidal, subharmonic “sinucose” and fundamental varicose, from the most to the least unstable [5]. The subharmonic “sinucose” mode corresponds to the case where the low-speed streaks, say, have the varicose shape while the surrounding high-speed streaks have a sinusoidal shape (or *vice-versa*). In the fundamental sinusoidal mode both type of streaks have the sinusoidal shape, while in the fundamental varicose they both have the varicose shape. We have succeeded in demonstrating both the fundamental sinusoidal and the subharmonic sinucose instability [7], although the latter is a lot less unstable than the former. We have not verified that the subharmonic sinucose does feedback on the streamwise rolls that generate the streaks but it is quite likely that it does. However, the sinusoidal mode is definitely the favored mode, just as in the case of a wake instability, and this strongly supports the idea that staggered vortices are the predominant structure [2, 3]. Nonetheless, we do not feel that there is any fundamental physical difference between the two types of structures, both result from the streaky flow instability, they simply correspond to different symmetries.

4 Discussion in response to other studies

One of our primary focus has been to dissect the self-sustaining process in order to identify its essential elements and to clearly demonstrate how one leads to the other in a closed cycle. In doing so, we have somewhat neglected to show the complete flow. This has led, apparently, to some confusion. In this section we respond to some statements made by Schoppa and Hussain [15] about our work.

One source of confusion has been the definition of “streamwise vortices”. Our definition above is clear: our “streamwise vortices” are x -independent. But there is also x -dependent streamwise vorticity contained in the 3D eigenmode that results from the streak instability. The vortices observed in visualization studies and in the educed coherent structures of course correspond to the sum of those various components. Indeed, the sum of the streaky base flow $[U(y, z), 0, 0]$ and the 3D streak eigenmode with a proper amplitude show wavy streaks similar to those observed near the wall ([6] Fig. 4 and [7] Fig. 2). Other results will be shown below.

Schoppa and Hussain [15], whose approach was entirely similar to that in [4], propose a mechanism based on a streak instability that sounds quite similar to the one we studied. They emphasize that theirs is an instability of “vortex-less” streaks, *i.e.* of a streaky flow of the form $[U(y, z), 0, 0]$ (see [15], eqn. (1) p. 399). But that is exactly the type of flow whose instabilities we have studied. The eigenmode analysis in [5, 6] is specifically formulated and performed for a flow of the form $[U(y, z), 0, 0]$. Although the main stability results in [4] were for a $[U(y, z), V(y, z), W(y, z)]$, the pure streaky flow, or “vortex-less” streaks, $[U(y, z), 0, 0]$ was considered explicitly, as stated in [4] end of Sect. 5. The conclusion was that it is the streaky flow that drives the instability, not the streamwise rolls. This *must* be the case, of course, given that the whole point of the process is that the rolls *receive* energy from the instability.

One difference between Schoppa and Hussain’s analysis and ours is that while their $U(y, z)$ is somewhat *ad hoc*, ours was generated by redistribution of the base shear by suitably chosen streamwise rolls. A key point is that we subsequently demonstrated that the nonlinear development of the streak instability generates streamwise rolls that are extremely close to those we picked initially [5, 6]. Schoppa and Hussain do not show that their flow returns sufficiently close to their starting point, the *ad hoc* vortex-less streaks $[U(y, z), 0, 0]$. Hence, they do not convincingly demonstrate self-sustenance. To demonstrate a self-sustaining cycle, one is free to choose whichever starting point but it is crucial to show that the flow returns to that arbitrary starting point. Otherwise, one just has one particular type of initial condition that leads to turbulence through a more or less clean transient evolution, but the mechanisms that sustain the turbulence may involve other key elements. The

emphasis on “vortex-less” streaks, for instance, pertains only to special initial conditions. Once the flow is in a self-sustained state, vortices are always present.

Schoppa and Hussain claim that their streak instability is distinct from the one we studied. They imply in their Sect. 3.3 that our instability is “localized to the streak flanks”. But that is incorrect as we have always focused on the fundamental sinusoidal mode. We have shown that the spanwise velocity for that mode has the form [5, 6]

$$w = e^{i\alpha x} (w_0(y) + w_1(y) \cos \gamma z + \dots) \quad (1)$$

The spanwise velocity is the dominant component and the first term in the z -expansion dominates [6]. The perturbation chosen by Schoppa and Hussain ([15], eqn. 2, p. 400), in fact has exactly the form of that first term. The sinusoidal mode goes right through the streaks. It is not at all “localized to the streak flanks”. It is clearly evident in Fig. 5 of [7] that the eigenmode is not localized to the streak flanks. The *varicose* mode would be localized to the streak flanks, but we have always focused on the more important sinusoidal mode whose first order term is not at all localized in z .

We note here that Schoppa and Hussain’s discussion of the *linear* streak instability mechanism in their Sect. 3.3 apparently calls on a nonlinear effect: “This differential \tilde{u}_x amplifies $\tilde{\omega}_x$ (...)”. This sounds like stretching of $\tilde{\omega}_x$ by $\partial_x \tilde{u}_x$ which is a nonlinear effect and thus cannot explain a linear mechanism. In their Sect. 4.3 they also call on vortex stretching, *i.e.* $\omega_x \partial_x u$ to explain the formation of “streamwise vortices”. That identification of $\omega_x \partial_x u$ as the dominant term coupled with their insistence on “vortex-less” streaks that have no ω_x and no $\partial_x u$ is somewhat confusing. Even if $\omega_x \partial_x u$ is the dominant term, the question then is where did that ω_x and $\partial_x u$ come from and what correlated them in the proper way?

A source of confusion is the definition of “streamwise vortices”. In order to demonstrate a complete self-sustaining process, and the return to the pure “vortex-less” streaks, one needs to consider the x -averaged streamwise velocity and vorticity. Studying the feedback from spatially localized snapshots of the full flow field may be misleading. When the x -average is considered, it is difficult to identify $\omega_x \partial_x u$ as the dominant term as, among other things,

$$\overline{\omega_x \partial_x u}^x = -\overline{u \partial_x \omega_x}^x.$$

To characterize the self-sustaining process, we have been led to decompose the flow into its x -dependent part and its x -average. The pure streaky flow $[U(y, z), 0, 0]$ is generated by pure streamwise rolls $[0, V(y, z), W(y, z)]$. The key part of the process is thus to study the feedback on those x -averaged rolls. We have considered the x -averaged equations with the Reynolds stresses that arise from the streaky flow

eigenmode [6, 7]. Our conclusions are that the x -averaged Reynolds stresses that include the u fluctuations, namely $\overline{uw^x}$ and $\overline{vw^x}$, do not contribute to the feedback on the rolls. Those Reynolds stresses appear in the equation for the x -averaged streamwise velocity $U(y, z)$. Their role is to extract energy from the streaks to sustain the linear streak instability. The Reynolds stresses that generate, or regenerate, the rolls are $\overline{uw^y}$, $\overline{vw^y}$ and $\overline{vw^x}$. All those Reynolds stresses arise from the instability of the streaky flow, as we have demonstrated explicitly [5, 6, 7].

Schoppa and Hussain do in fact consider the x -average flow when discussing regeneration and their Fig. 13 is very similar to one half of our Fig. 13 in [4] (see also our discussion in [7] Sect. 2.3). In the periodic plane Couette geometry, there is an extra set of streaks on the 2nd wall, shifted by half a wavelength in the z -direction. There are contributions to the regeneration of streamwise rolls from both walls but the mechanisms are clearly identical. In conclusion, if their process is driven by the 3D instability of “vortex-less” streaks entirely analogous to our streaky flow $[U(y, z), 0, 0]$ instability and the feedback on the x -averaged vorticity which is the “heart of their process” is also entirely analogous to the feedback that we studied, then we do not see any “fundamental differences” between the two processes.

We will not respond in detail to Schoppa and Hussain’s Sect. 5.3 in which they consider the *short time evolution from special initial conditions*. This does not seem relevant to the discussion of a *self-sustaining process* that leads to non-trivial attractors for the flow. Our DNS studies [4] clearly demonstrate the self-sustaining process but to isolate it in its cleanest form we had to start from higher Reynolds number turbulence and carefully track the “turbulent” flow to lower Reynolds number. At very low Reynolds numbers, the basin of attraction of the non-trivial states maybe small and difficult to reach through time-evolution from arbitrary initial conditions. We note however that Schoppa and Hussain’s comparison of their Fig. 16f to their Fig. 8c is not appropriate. The comparison should be made between the *lower half* of their 16a to their 8a and the lower half of 16b to their 8c. Those figures both correspond to evolution from “vortex-less” streaks and to the same times, 17^+ and 103^+ , respectively. Figure 16f does not correspond to the same type of initial conditions nor to the same time as Fig. 8c. When the appropriate figures are compared, there is in fact a definite similarity. The plane Couette evolution is cleaner however.

That was precisely the reason for considering plane Couette flow at very low Reynolds number in a small periodic box. Our goal is to clearly isolate a complete self-sustaining process, not to explain every feature of the spatio-temporal disorder that is observed in the near-wall region of turbulent shear flows. The “inactive motions” are largely suppressed in our very constrained situation. The presence of a second viscous wall further

limits inactive motions *as well as* the self-sustaining process, unless the process were of viscous origin, such as the Tollmien-Schlichting type of instability or the viscous rebound mechanism [17]. Further work using free-slip and imposed stress boundary conditions show that the mechanism is NOT of viscous origin [6].

5 Exact sustained states

In this section we demonstrate the validity and relevance of the self-sustaining process sketched in Fig. 2, in a different and more definite way, by constructing exact sustained states. We focus on steady state solutions and consider plane Couette flow with (Neumann) stress boundary conditions instead of the usual (Dirichlet) velocity boundary conditions. This is partly for “historical” reasons: the derivation of low-order models is simpler for free-slip boundary conditions where Fourier modes can be used in all directions and this work is a continuation of that work [6]. There are also interesting physical reasons to consider imposed stress: viscous instabilities of the Tollmien-Schlichting kind do not occur [16] and the viscous rebound mechanism [17] cannot operate.

To calculate exact steady state one is faced with finding solutions to a large system of nonlinear equations – the steady Navier-Stokes equations. The basic approach to do this is Newton’s method. The key to this approach is to generate a good initial guess for the Newton iteration, otherwise the iterations do not converge or they converge to spurious states. We construct such an initial guess based on the self-sustaining process and the mean-field approach suggested in [5, 6], where the mean field consists of the x -averaged flow $[U(y, z), V(y, z), W(y, z)]$. The mean field is constructed by picking the weakest streamwise rolls $[0, V(y, z), W(y, z)]$ that generate the largest streaks, holding the rolls steady and calculating the corresponding steady streaky flow $[U(y, z), 0, 0]$. Next, a linear stability analysis of that x -independent flow is performed to determine the streamwise wavenumber α corresponding to a *neutral* eigenmode. The final step is to select the amplitude of that neutral mode in order to sustain the steady streamwise rolls. This procedure generates an approximate steady state.

This general idea can be turned into a smooth continuation strategy by introducing an explicit steady external forcing for the rolls. Thus an explicit forcing of the form

$$\frac{F_r}{R^2} \frac{(\beta^2 + \gamma^2)}{\gamma} \begin{pmatrix} 0 \\ \gamma \cos \beta y \cos \gamma z \\ \beta \sin \beta y \sin \gamma z \end{pmatrix}, \quad (2)$$

where $\beta = \pi/2$, is added to the Navier Stokes equations with imposed stress boundary conditions. The forcing is chosen such that a maximum vertical velocity of F_r/R occurs at $y = z = 0$. Steady state solutions are then

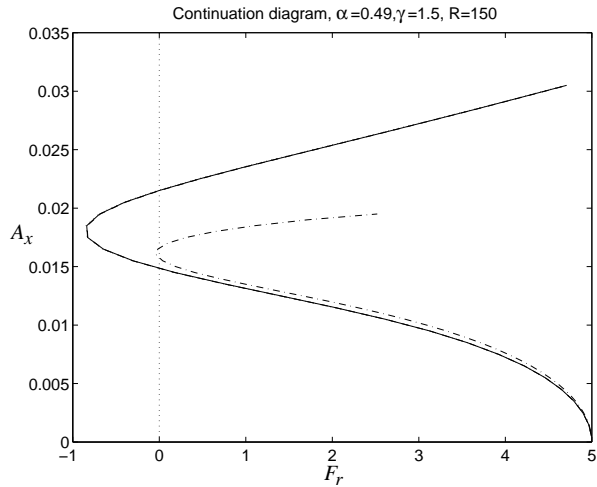


Figure 5: Tracking of an exact steady state from $F_r = 5$, $A_x = 0$ to $F_r = 0$, $A_x \neq 0$. Three resolutions are plotted: $L_T \times M_T \times N_T = 7 \times 19 \times 7$ (dot), $8 \times 20 \times 8$ (dash) and $9 \times 21 \times 9$ (solid). The vertical dotted line highlights $F_r = 0$. The dash-dot curve is for $L_T \times M_T \times N_T = 1 \times 21 \times 9$.

tracked in the $A_x - F_r$ plane, where A_x is a measure of the amplitude of the x -dependent fluctuation, starting from the $A_x = 0$ point where a neutral mode exists to a finite amplitude solution where $F_r = 0$ and $A_x \neq 0$. Here A_x is taken as the root-mean-square amplitude of the purely spanwise $(\alpha, 0, 0)$ mode. This corresponds to the amplitude of the first term in eqn. 1.

The formulation is a direct extension of that presented in [6] Sect. III A and imposes all symmetries discussed therein. The channel goes from $y = -1$ to $y = 1$. The Reynolds number R is based on the half-channel width h and the half wall velocity difference $U_w = u_*^2 h / \nu$ of the laminar flow $U(y) = u_*^2 y / \nu$, thus $R = U_w h / \nu = u_*^2 h^2 / \nu^2 = R_*^2$, where ν is the kinematic viscosity and $u_* = (\nu |dU/dy|_w)^{1/2}$ is the friction velocity. Fourier expansions are used in all directions with L_T , M_T and N_T modes in the x , y and z directions, respectively. Various truncation rules have been used. The results shown herein are for an elliptical truncation which omits any mode whose wavenumber index (l, m, n) is such that

$$\left| \frac{l}{L_T + 1} \right|^2 + \left| \frac{m}{M_T + 1} \right|^2 + \left| \frac{n}{N_T + 1} \right|^2 \geq 1. \quad (3)$$

The Fourier expansion is not spectrally accurate as $M_T \rightarrow \infty$ for imposed stress boundary conditions (the rate of convergence is probably $O(M_T^{-4})$) but for the low resolution to which we are limited, the Fourier approach may in fact be more accurate than one based on Chebyshev expansions. This was verified by experimentation with a related equation (the linear eigenvalue problem for the vertical vorticity). Related problems have been considered where the imposed stress boundary condi-

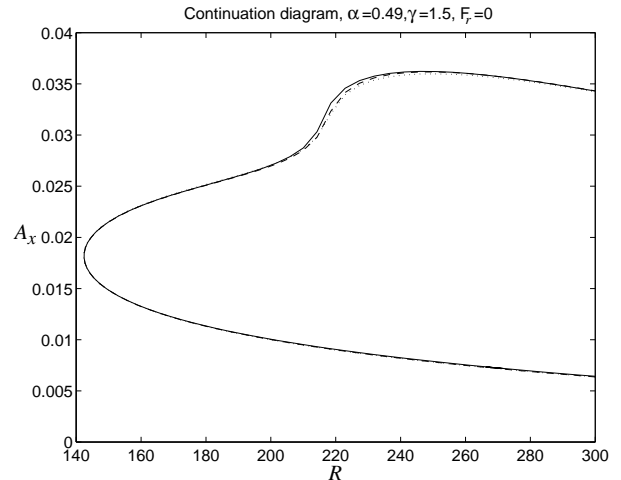


Figure 6: Tracking of an exact steady state for $F_r = 0$. Three resolutions are plotted: $L_T \times M_T \times N_T = 7 \times 19 \times 7$ (dot), $8 \times 20 \times 8$ (dash) and $9 \times 21 \times 9$ (solid).

tions are replaced by no-stress boundary conditions together with an explicit smooth forcing $F(y)\hat{x}$, localized near the wall, in which case the Fourier expansion is spectrally accurate. Imposed stress can be represented by the explicit forcing $F(y) = 2R^{-1}[\delta(y-1) - \delta(y+1)]$ with zero stress boundary conditions. The results for such problems are essentially identical to those shown here for imposed stress boundary conditions as long as $F(y)$ is sufficiently localized near the walls. The results are shown for 3 different truncations: $L_T \times M_T \times N_T = 7 \times 19 \times 7$, $8 \times 20 \times 8$ and $9 \times 21 \times 9$ which correspond to 1327, 1764 and 2294 degrees of freedom, respectively, after reduction from the symmetries.

For $R = 150$, $F_r = 5$ and $\gamma = 1.5$, the steady streamwise flow $[U(y, z), V(y, z), W(y, z)]$ is neutrally stable at $\alpha = 0.49$. Increasing A_x up from zero reduces the external forcing F_r required to sustain the rolls and an exact steady state, as shown in Fig. 5. This again demonstrates that the nonlinear self-interaction of the $e^{i\alpha x} \vec{v}(y, z) + c.c.$ sinusoidal streak mode directly feeds back onto the rolls. As A_x is increased away from zero, the nonlinear self-interaction terms takes over the sustenance of the rolls from the explicit forcing F_r . The parabolic shape of the curve in Fig. 5 near $F_r = 5$, $A_x = 0$, where $F_r = 5 - O(A_x^2)$ confirms that this is a first order nonlinear effect. The dash-dot curve in Fig. 5 corresponds to a “Mean Flow-First Harmonic” theory which includes only one $e^{i\alpha x}$ mode. As A_x further increases, higher order nonlinear effects come in and at $F_r = 0$ there are two possible steady states. These states can serve as starting points for continuation of solutions in the $R - A_x$ plane, with F_r now identically zero, of steady state solutions of the Navier-Stokes equations with imposed stress boundary conditions. This $R - A_x$ curve is shown in Fig. 6. In the pure shear flow ($F_r = 0$), the steady states arise from a *saddle-node* bi-

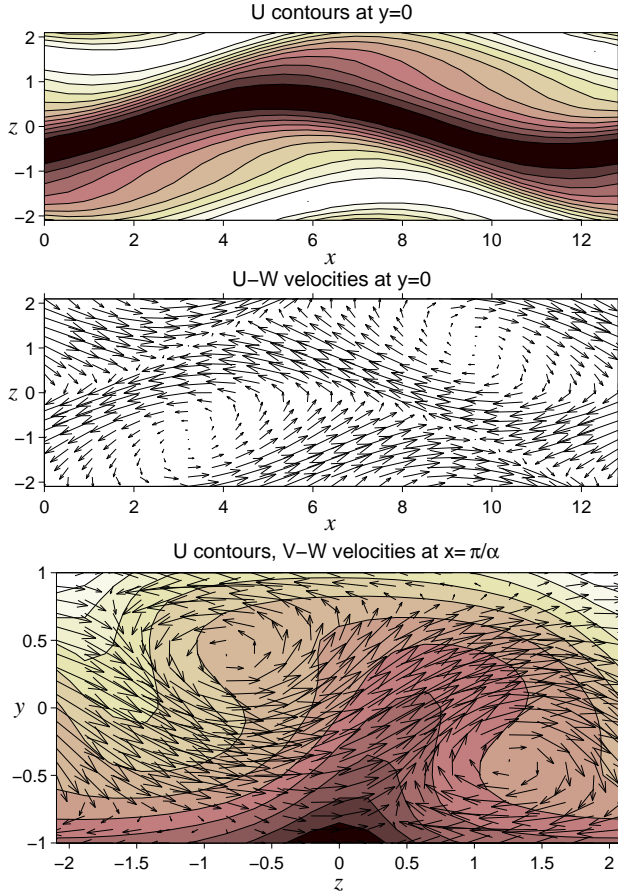


Figure 7: Cuts through exact upper branch steady solution at $R = 150$, $\alpha = 0.49$, $\gamma = 1.5$. Compare xz cuts to ‘Plan View’ in Fig. 1 and yz cut to ‘Section XX’ in Fig. 1.

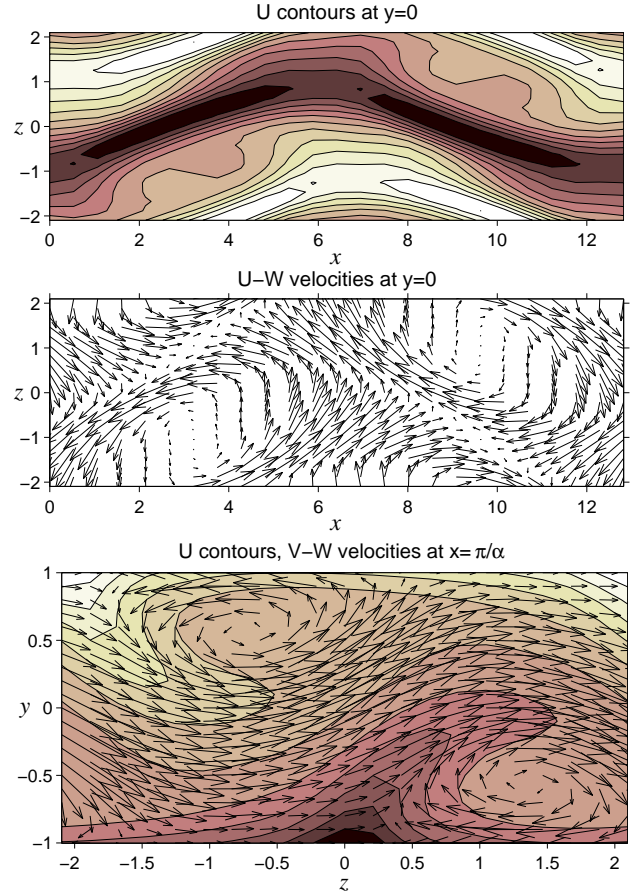


Figure 8: Cuts through exact upper branch steady solution at $R = 300$, $\alpha = 0.49$, $\gamma = 1.5$. Compare xz cuts to ‘Plan View’ in Fig. 1 and yz cut to ‘Section XX’ in Fig. 1.

furcation (near $R_c = 140$ for $\alpha = 0.49$, $\gamma = 1.50$), much as for the simple ODE $\dot{u} = (R - R_c) - u^2$ that has no fixed point for $R > R_c$ and 2 fixed points when $R < R_c$.

The structure of the upper branch solution (*i.e.* the solution with largest A_x) is shown in Fig. 7 for $R = 150$ and in Fig. 8 for $R = 300$. The lower branch solutions have similar structure with stronger streaks but weaker x -waviness. The similarity between these steady states and the educed coherent structures is striking. The solutions consists of wavy streaks flanked with staggered vortices inclined in the streamwise direction. The figures are almost identical to those obtained for the ensemble-averaged coherent structures. This close similarity between the exact steady states and the educed coherent structures is quite remarkable given that the coherent structures were educed from a turbulent channel flow with no-slip boundary conditions at $R_* = 180$ while the steady states shown in Fig. 7 and Fig. 8 correspond to a plane Couette flow geometry with stress boundary conditions at $R_* = 24.5$ and $R_* = 34.6$, respectively, where these R_* are based on the full channel width for the plane Couette geometry and the half-width for Poiseuille flow. The mean shear for the upper

branch solution at $R = 150$ and $R = 300$ is compared to the trivial laminar flow $U(y) = y$ in Fig. 9. The maximum velocity is significantly reduced for those 3D steady states in spite of the low Reynolds numbers.

Similar steady state solutions exist for the regular plane Couette flow with no-slip boundary conditions. Such solutions have been calculated by other authors, either by continuation of wavy Taylor-Couette vortices in rotating plane Couette flow [11, 18] or of wavy convection rolls in sheared convection [12]. The exact nature of the boundary conditions, imposed velocity or imposed stress, thus does not have much effect on the steady states. This is probably because the self-sustaining process responsible for those solutions is non-linear and is not of viscous origin. In fact, the present evidence is that even the critical Reynolds numbers for existence of the 3D steady states are very close, within 10% of each other, for both types of boundary conditions. In contrast, the critical Rayleigh number in Rayleigh-Bénard convection with free-slip boundary conditions is about 657 and thus significantly different from the critical value of 1708 with no-slip boundary conditions.

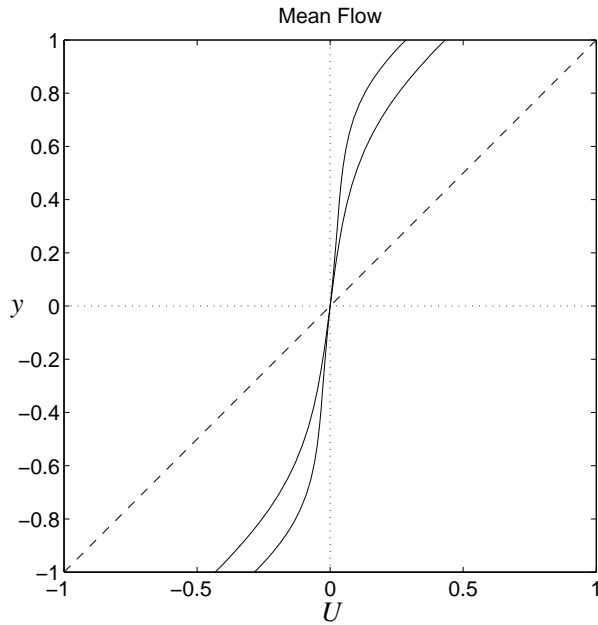


Figure 9: Mean flow $\bar{U}(y)$ for upper branch steady state at $R = 150$ (largest solid) and at $R = 300$ (smallest solid) compared with trivial steady state $U(y) = y$ (dashed).

6 Conclusions

A self-sustaining process (Fig. 2) that we have studied in a series of earlier publications has been briefly reviewed. The similarities and differences with processes studied by other authors have been discussed. We have responded to several misleading statements about our work made by Schoppa and Hussain in their position paper [15]. Exact sustained states, in the form of 3-dimensional steady states, have been calculated for the Navier-Stokes equations using a continuation approach that is directly based on the self-sustaining process. These exact states are remarkably similar to the coherent structures deduced from DNS data in plane Poiseuille flow and provide strong evidence for the validity and relevance of the self-sustaining process.

References

- [1] Self-Sustaining Mechanisms of Wall Turbulence, Panton (ed.), Computational Mechanics Publication, Southampton UK and Boston USA, 1997.
- [2] D.D. Stretch, "Automated pattern eduction from turbulent flow diagnostics," *Annual Research Briefs-1990*, Center for Turbulence Research, Stanford U.
- [3] J. Jeong, F. Hussain, W. Schoppa & J. Kim "Coherent structures near the wall in a turbulent channel flow," *J. Fluid Mech.* **332**, 185-214 (1997).
- [4] J. M. Hamilton, J. Kim and F. Waleffe, "Regeneration mechanisms of near-wall turbulence structures," *J. Fluid Mech.* **287**, 317, 1995.
- [5] F. Waleffe, "Hydrodynamic stability and turbulence: beyond transients to a self-sustaining process," *Studies in Appl. Math.*, **95**, 319-343 (1995).
- [6] F. Waleffe, "On a self-sustaining process in shear flows," *Phys. Fluids* **9**, 883, 1997.
- [7] F. Waleffe & J. Kim, "How streamwise rolls and streaks self-sustain in a shear flow," in [1] pp. 309-332.
- [8] D.J. Benney, "The evolution of disturbances in shear flows at high Reynolds numbers," *Stud. Appl. Math.* **70**, 1-19 (1984).
- [9] R.F. Blackwelder, "An Experimental Model for Near-Wall Structure," in [1] pp. 49-64.
- [10] Malkus, W.V.R. and Zaff, D.B. 1987 (see Zaff's thesis, MIT Department of Mathematics, 1987).
- [11] M. Nagata "Three-dimensional finite-amplitude solutions in plane Couette flow: bifurcation from infinity," *J. Fluid Mech.* **217**, 519-527 (1990).
- [12] Clever, R.M. and Busse, F.H. "Three-dimensional convection in a horizontal layer s ubjected to constant shear," *J. Fluid Mech.* **234**, 511-527 (1992).
- [13] M.T. Landahl, "On Sublayer Streaks," *J. Fluid Mech.* **212**, 593-614 (1990).
- [14] M. S. Acarlar and C. R. Smith, "A study of hairpin vortices in a laminar boundary layer. Part II: hairpin vortices generated by fluid injection," *J. Fluid Mech.* **175**, 43, 1987.
- [15] W. Schoppa & F. Hussain, "Genesis and Dynamics of Coherent Structures in Near-wall Turbulence: A New Look," in [1] pp. 385-422.
- [16] Lou Howard has proven stability under no-stress boundary conditions for $U(y) = y, 1 - y^2$ and $\sin \pi y/2$ (September 1997, private communication).
- [17] J. Jimenez & P. Orlandi "The rollup of a vortex layer near a wall," *J. Fluid Mech.* **248**, 297 (1993).
- [18] A. Conley, "New plane shear flows," *Ph.D. Thesis, California Institute of Technology*, H. B. Keller, advisor (1994).